Activity determination of 60Co and the importance of its beta spectrum

Karsten Kossert, Justyna Marganiec-Galazka, Xavier Mougeot, Ole J. Naehle

HAL Id: cea-01799862

https://cea.hal.science/cea-01799862

Submitted on 11 Feb 2020
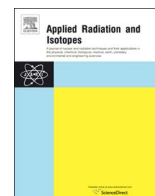
Activity determination of ^{60}Co and the importance of its beta spectrum

Karsten Kossert[a],[*], Justyna Marganiec-Gałązka[a], Xavier Mougeot[b], Ole J. Nähle[a]

[a] Physikalisch-Technische Bundesanstalt (PTB), Bundesallee 100, 38116 Braunschweig, Germany
[b] CEA, LIST, Laboratoire National Henri Becquerel, F-91191 Gif-sur-Yvette, France

HIGHLIGHTS

- The activity of ^{60}Co was measured using four methods.
- $4\pi\beta$-γ coincidence counting and liquid scintillation counting (LSC) was used.
- Results of LSC depend on the computed beta spectra.
- Discrepancies were resolved with improved beta spectra calculations.
- The atomic exchange effect and screening corrections matter.

ARTICLE INFO

ABSTRACT

The activity concentration of a ^{60}Co solution was measured by means of two $4\pi\beta$-γ coincidence counting systems using a liquid scintillation counter and a proportional counter (PC) in the beta channel, respectively. Additional liquid scintillation measurements were carried out and CIEMAT/NIST efficiency tracing as well as the triple-to-double coincidence ratio (TDCR) methods were applied to analyse the data. The last two methods require computed beta spectra to determine the counting efficiencies.

The results of both $4\pi\beta$-γ coincidence counting techniques are in very good agreement and yield a robust reference value. The initial activity concentration determined with liquid scintillation counting was found to be significantly lower than the results from $4\pi\beta$-γ coincidence counting. In addition, the results from TDCR and CIEMAT/NIST show some inconsistency.

The discrepancies were resolved by applying new beta spectrum calculations for the dominant allowed beta transition of ^{60}Co. The use of calculations which take screening effects as well as the atomic exchange effect into account leads to good agreement between all four methods; the combination of these techniques delivers an important validation of beta spectra.

1. Introduction

In previous work, it was demonstrated that the calculated beta spectra are extremely important when employing liquid scintillation (LS) counting for primary activity determination. Using inappropriate beta spectra may lead to discrepancies when varying the counting efficiency and may also lead to discrepancies between the activity concentration derived from CIEMAT/NIST efficiency tracing and TDCR, respectively. When studying ^{63}Ni (Kossert and Mougeot, 2015), such discrepancies were only resolved when the beta spectrum computation takes atomic screening and exchange effects into account (Mougeot and Bisch, 2014).

For ^{241}Pu, the agreement between the two LS methods was improved by Kossert et al. (2011) when using the best experimentally determined beta spectrum available at that time. The experimental result was obtained from

Loidl et al. (2010) using high-precision measurements by means of modern cryogenic metallic calorimeters. Since their publication, the quality of published beta spectra have been improved with both theoretical calculations (Mougeot et al., 2012; Mougeot and Bisch, 2014) and experimental determination by means of cryogenic detectors (Loidl et al., 2014).

In this work, ^{60}Co ($T_{1/2}$ = 5.2711 (8) a; Bé et al., 2006) was studied using various methods. Cobalt-60 decays by β^- emission which is – in most cases - accompanied by two coincident γ transitions (Bé et al., 2006) which makes it an ideal candidate for coincidence counting techniques (Schönfeld et al., 2002). A simplified decay scheme is shown in Fig. 1. The activity concentration of a ^{60}Co solution was measured by means of $4\pi\beta(LS)$-γ coincidence counting with an LS counter in the beta channel. Currently, this technique is being developed as a new activity standardization method at PTB. Validation measurements were carried out with a revived $4\pi\beta$-γ
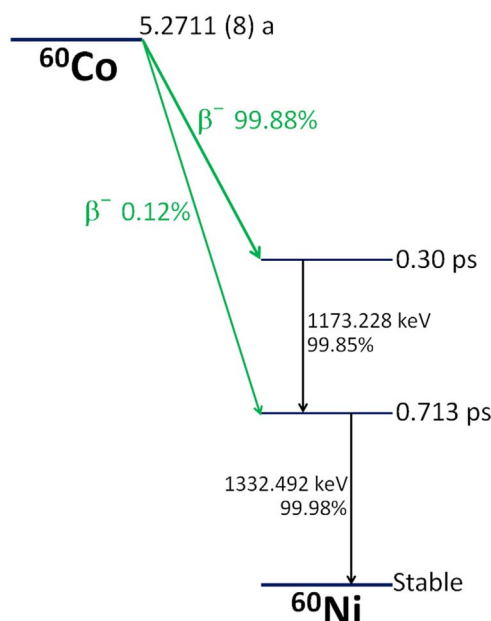

Fig. 1. Simplified decay scheme of ^{60}Co.

coincidence counting system with a PC in the beta channel.

Additional measurements were carried out using liquid scintillation counters with two and three photomultiplier tubes. The counting efficiencies for these systems were determined using CIEMAT/NIST efficiency tracing and the TDCR method (Broda et al., 2007). Both methods require computed beta spectra and other nuclear decay data as input data.

The results of both $4\pi\beta$-γ coincidence counting techniques are in very good agreement and their results do not depend on the beta spectrum calculation. In contrast to coincidence counting, the TDCR method and CIEMAT/NIST efficiency tracing yield results which depend to a certain extent on the above-mentioned input data. In a first analysis, activity concentrations determined with these techniques were found to be systematically lower than the results from $4\pi\beta$-γ coincidence counting. Moreover, a significant discrepancy between results from TDCR and CIEMAT/NIST was noticed. These discrepancies were resolved by applying new beta spectrum calculations for the allowed beta transition of ^{60}Co which take screening effects as well as the atomic exchange effect into account. With this computation, results of the LS methods are consistent even when applying efficiency variation over a wide efficiency range.

Thus, the combination of techniques allows an important validation of calculated and measured beta spectra. Improvements for beta spectra measurements as well as for the corresponding calculation techniques are main tasks in the ongoing EMPIR project MetroBeta.

The uncertainties as well as the advantages and disadvantages of the methods are discussed in detail. All uncertainties stated in this work are standard uncertainties (coverage factor $k = 1$).

2. Experimental details

The measurements were performed using an aqueous ^{60}CoCl$_2$ solution containing 50 µg inactive CoCl$_2$ per g of solution that is 0.1 mol L^{-1} with respect to HCl. A preliminary activity concentration of about 143.4 kBq g^{-1} on the reference date (1st January 2015, 0 h CET) was calculated from a gravimetrically determined dilution factor and from the activity concentration of a master solution. The activity concentration of the master solution was determined by means of a calibrated ionization chamber. The corresponding calibration factor can be traced back to $4\pi\beta$(PC)-γ coincidence counting and was determined more than 30 years ago. Since then, the calibration factor has been confirmed by further primary standardizations several times (Schönfeld

et al., 2002).

The master solution was also measured by γ-ray spectrometry and no γ-emitting radioactive impurities were found.

2.1. Sample preparation

The LS samples were prepared with 15 mL Ultima Gold™ scintillator in 20 mL low-potassium borosilicate glass vials. About 0.97 mL of distilled water were filled into the vials before adding weighed portions of about 30 mg of the ^{60}Co solution. Nitromethane (CH$_3$NO$_2$) was used to vary the counting efficiencies. Altogether, 6 LS samples were prepared. One of the samples was prepared with 15 mL Ultima Gold™ scintillator and 1 mL of distilled water but without any radioactive material. This sample was used to measure the background counting rates, which were then subtracted.

Two sources were prepared for $4\pi\beta$(PC)-γ-counting. The sources were very thin VYNS (polyvinyl chloride-polyvinyl acetate copolymer) foils (15 µg cm^{-2}) that were coated with a thin layer of an Au-Pd alloy (15 µg cm^{-2}) on each side and mounted on stainless steel rings. The foils were pre-treated by electrospraying them with a colloidal SiO$_2$ suspension on a circular area of about 6 mm in diameter. Finally, weighed aliquots of the ^{60}Co solution were deposited on the centre of the sources which were then slowly dried under a cover to prevent dust particles falling onto the sources. A background sample was prepared without any radioactive material.

The masses of about 15 mg of the ^{60}Co solution deposited into the LS vials or on a single VYNS source were determined by difference weighing of a pycnometer before and after drop deposition. The masses of all samples as well as the dilution factor were determined gravimetrically using two Mettler balances traceable to the German national mass standard.

2.2. $4\pi\beta$(LS)-γ coincidence measurements

The $4\pi\beta$(LS)-γ coincidence system comprises a TDCR counter with an automated sample changer and a cylindrical NaI scintillation detector (102 mm × 102 mm) below the optical chamber of the LS system. The amplified and discriminated anode signals from the three Hamamatsu R331-05 PMTs are fed into an FPGA-based coincidence unit referred to as the 4KAM module (Nähle et al., 2014). More details about the $4\pi\beta$(LS)-γ coincidence system, its electronics and the signal treatment are described by Marganiec-Gałązka et al. (2017).

In this work, the common extendable dead time of the 4KAM module was adjusted to 30 µs. The coincidence resolving times were defined as 77.5 ns and 76.5 ns for the beta channel (3 PMTs of the LS system) and for the β-γ coincidences, respectively.

The energy window in the gamma channel was adjusted using a single channel analyzer (SCA) module (ORTEC SCA 551). Three different settings were used: 1) an open window to cover the whole energy spectrum, 2) a window to cover the full-energy peak at 1173 keV, and 3) a window to cover the two dominant full-energy peaks at 1173 keV and 1332 keV.

The coincidence counting technique requires an efficiency variation over a wide range and subsequent extrapolation of data (see below). At PTB, the amount of nitromethane is usually less than 50 µL which defines a lower limit of the covered efficiency range. To extend the efficiency range, thin neutral density (ND) filters (LEE Filters Worldwide, Hampshire, UK) with light transmission from 69.3% to 6.6% were used in addition to chemical quenching (for details see Marganiec-Gałązka et al., 2017). Each source was measured several times with different ND filters to cover the required efficiency range.

When measuring radionuclides with high-energy gamma-ray emissions, the background can be increased when several samples are stored in the sample changer system, i.e. close to the optical chamber and the NaI detector. The distance from the optical chamber is rather small in some commercial LS counters and – in such a case – the measured

background can be considered non-representative (see Section 2.4). The custom-built $4\pi\beta(LS)$-γ coincidence system, however, ensures a large distance and massive lead shielding between the sensitive detector components and other LS sources. Thus, any bias in the background was found to be negligible for the ^{60}Co measurements discussed in this work.

2.3. $4\pi\beta(PC)$-γ coincidence measurements

The VYNS sources were measured in a $4\pi\beta$-γ coincidence system equipped with a pillbox-type PC filled with pure (99.95%) methane under atmospheric pressure. The photons were counted by means of a cylindrical 75 mm × 75 mm NaI(Tl) detector above and a cylindrical 100 mm × 100 mm Na(Tl) below the PC. Thus, two measurements with different settings in the gamma channel can be carried out simultaneously. In the following, the two NaI detectors are referred to as G1 and G2, respectively. The analogue signal processing was accomplished by means of a preamplifier, an amplifier and an SCA, after which an artificial, non-extendable dead time of about 8 μs was introduced by means of high-precision dead time units (Schönfeld and Janssen, 1994). A delay unit was used to minimise the delay between the gamma and beta channels. The digital outputs of gamma and beta channels were fed into coincidence units with a resolving time of about 1 μs. The counting rates were corrected for background and nuclear decay and analysed on the basis of the expression given by Smith (1978) for the coincidence counting rate (see also ICRU Report 52, 1994).

A discriminator was used to adjust the threshold above the noise level in the beta channel. In the gamma channels two different settings were used. In the first setting the whole gamma spectrum was accepted and in the second setting the energy range was defined to include the full-energy peaks of the dominant peaks at 1173 keV and 1332 keV as used for $4\pi\beta(LS)$-γ coincidence counting (see Section 2.2). The beta counting efficiency was varied by successive addition of VYNS absorption foils.

The measurement system is equipped with an automated sample changer which was used to carry out many measurements of the background sample as well as of the ^{60}Co samples with varying beta counting efficiency. Again, massive lead shielding and a large distance between sources and detectors ensure that a potential bias of background is negligible.

2.4. CIEMAT/NIST measurements

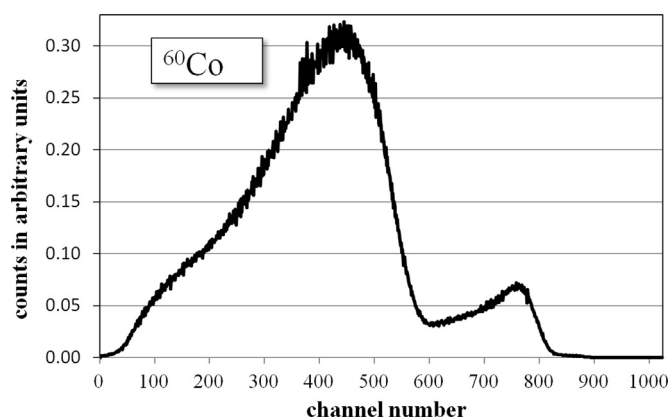The LS samples were measured in a Wallac 1414 Guardian™ liquid scintillation spectrometer. Fig. 2 shows a measured liquid scintillation spectrum obtained with this apparatus. The calibration curve, i.e. the counting efficiency of ^{3}H as a function of the quenching indicator SQP (E), was measured with the aid of a PTB standard solution of ^{3}H. The LS samples containing ^{3}H have the same sample composition and geometry as the ^{60}Co LS samples.

The Wallac counter is equipped with an automated sample changer and the LS vials are located in a rack. The sample to be measured is moved upwards into the optical chamber with an elevator stick and the rack with other samples stays in a constant position. In this configuration, neighbouring samples are at a close distance from the optical chamber and the PMTs. For high-energy gamma emissions – such as in the case of ^{60}Co decay - this can lead to additional background events and the measured background is not representative any more. It is to be noted that some samples can have two radioactive neighbouring samples while others have only one. To get rid of this problem and to avoid the necessity of additional corrections, the ^{60}Co samples and the background sample were measured without any neighbours, i.e. only one sample was placed in the rack while all other samples were stored outside the counter system. Results can be biased by more than 0.1% when ignoring this effect.

2.5. TDCR measurements

The LS samples were measured in two custom-built TDCR systems of PTB. The first system makes use of the MAC3 coincidence module (Bouchard and Cassette, 2000) with 40 ns coincidence resolving time and was described by Nähle et al. (2010). The second system is a new LS-γ counter with an automated sample changer as described in Section 2.2. For the (pure) TDCR measurements, the coincidence resolving time in this system was about 76.5 ns. Further details about the counters and general adjustments are described by Nähle et al. (2010) and Marganiec-Gałązka et al. (2017).

3. Analysis of data from $4\pi\beta(LS)$-γ and $4\pi\beta(PC)$-γ coincidence counting

The counting rates of beta events N_β, gamma events N_γ and β-γ coincidences events N_c were used to plot the ratio: $\frac{N_\beta \cdot N_\gamma}{N_c}$ as a function of

$$x = \frac{\left(1 - \frac{N_c}{N_\gamma}\right)}{\left(\frac{N_c}{N_\gamma}\right)}.$$ Polynomial functions $f(x)$ were fitted to the data by means of the least-squares method and the function was finally extrapolated to $\left(\frac{N_c}{N_\gamma}\right) = 1$, which corresponds to a beta efficiency $\varepsilon_\beta = 100\%$ (Figs. 3 and 4).

For $4\pi\beta(LS)$-γ coincidence counting, the β counting rate was defined either as the counting rate for the logical sum of double coincidences, N_D, or as the counting rate for triple coincidences, N_T. For $4\pi\beta(PC)$-γ coincidence counting, two different γ counters G1 and G2 (see Section 2.3) were used. Thus, various experimental data sets are available for the extrapolation procedure. In addition, different γ window settings were applied as described in Sections 2.2 and 2.3. The activity concentrations of various extrapolations are listed in Table 1. The relative deviation between the highest and the lowest result was found to be less than 0.2%.

Fig. 3 shows two examples of the extrapolation for $4\pi\beta(LS)$-γ coincidence counting. In both cases, the counting rate N_D was used as a beta counting rate. An open gamma window (left side of Fig. 3) or a gamma window that includes only the region of the two dominant full-energy peaks at 1173 keV and 1332 keV (right side of Fig. 3) was selected in the gamma channel. The results from the corresponding extrapolation method are in good agreement (see Table 1), although the extrapolation curves have slopes with opposite signs. In the case of $4\pi\beta(LS)$-γ coincidence counting, second order polynomial functions were used for the extrapolation. However, first order polynomials were

Fig. 2. Measured LS spectrum of ^{60}Co. The measurement was carried out in a Wallac 1414 counter with logarithmic amplification. A background spectrum has been subtracted. For both measurements other ^{60}Co samples were removed from the sample changer system in order to avoid additional background events.

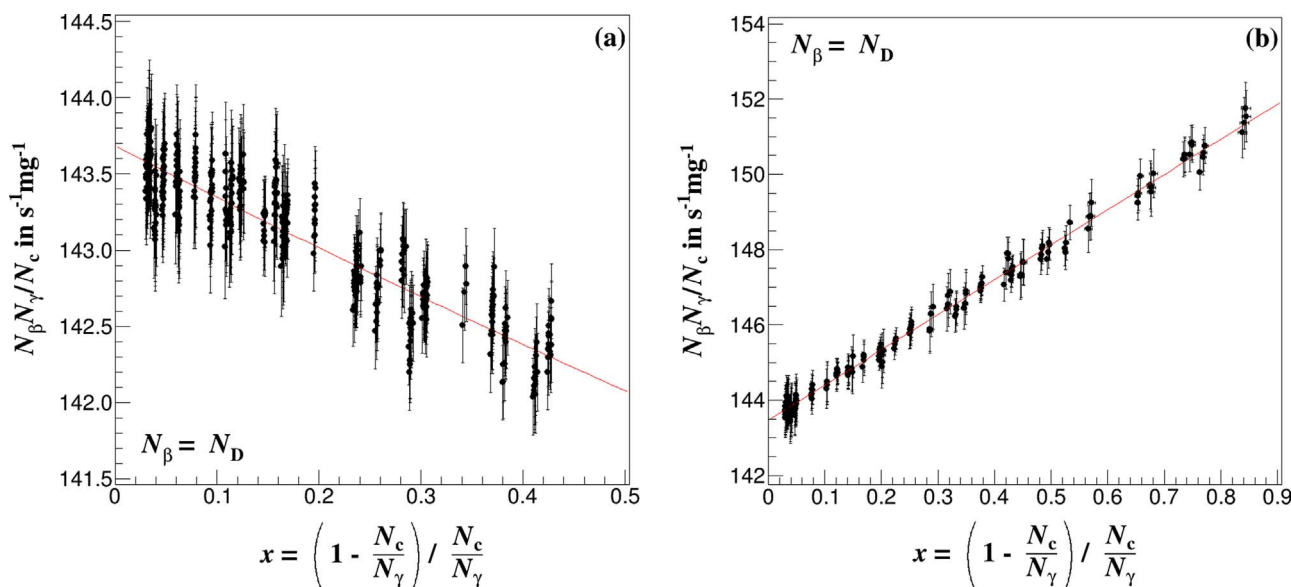**Fig. 3.** $\frac{N_\beta \cdot N_\gamma}{N_c}$ measured with a 4πβ(LS)-γ coincidence system as a function of $x = \frac{\left(1 - \frac{N_c}{N_\gamma}\right)}{\left(\frac{N_c}{N_\gamma}\right)}$; function $f(x)$ is a 2nd degree polynomial which was fitted to the experimental data, and the bars represent the statistical uncertainty of the individual data. In the left figure an open γ window was used, whereas the γ window was limited to the region of the two dominant peaks at 1173 keV and 1332.5 keV in the right figure. For the plots the counting rate of double coincidences N_D was used as β counting rate ($N_\beta = N_D$).

also applied to estimate uncertainties.

Corresponding examples of the extrapolation of experimental data from 4πβ(PC)-γ coincidence counting are shown in Fig. 4. In this case, first order polynomials were used as extrapolation functions. Second order polynomials were also applied to evaluate uncertainties.

The statistical uncertainties of individual data points were used as weighting factors for the fitting procedures. However, the results were almost identical to the values which were obtained with unweighted fits. Since the individual results of each method are highly correlated, the activity concentrations for each setup were calculated as the arithmetic mean. The following results were obtained from the two methods:

4πβ(PC)-γ coincidence counting: $a = (143.61 \pm 0.34)$ kBq g^{-1} and 4πβ(LS)-γ coincidence counting: $a = (143.50 \pm 0.47)$ kBq g^{-1}. The reference date was defined as 1st January 2015, 0 h CET.

Detailed uncertainty budgets are shown in Table 2. The uncertainty components related to dead time and coincidence resolving time were conservatively estimated in the case of 4πβ(LS)-γ coincidence counting. The 4KAM module uses different techniques to determine the coincidences for the beta channels (D and T) and β-γ coincidences. The
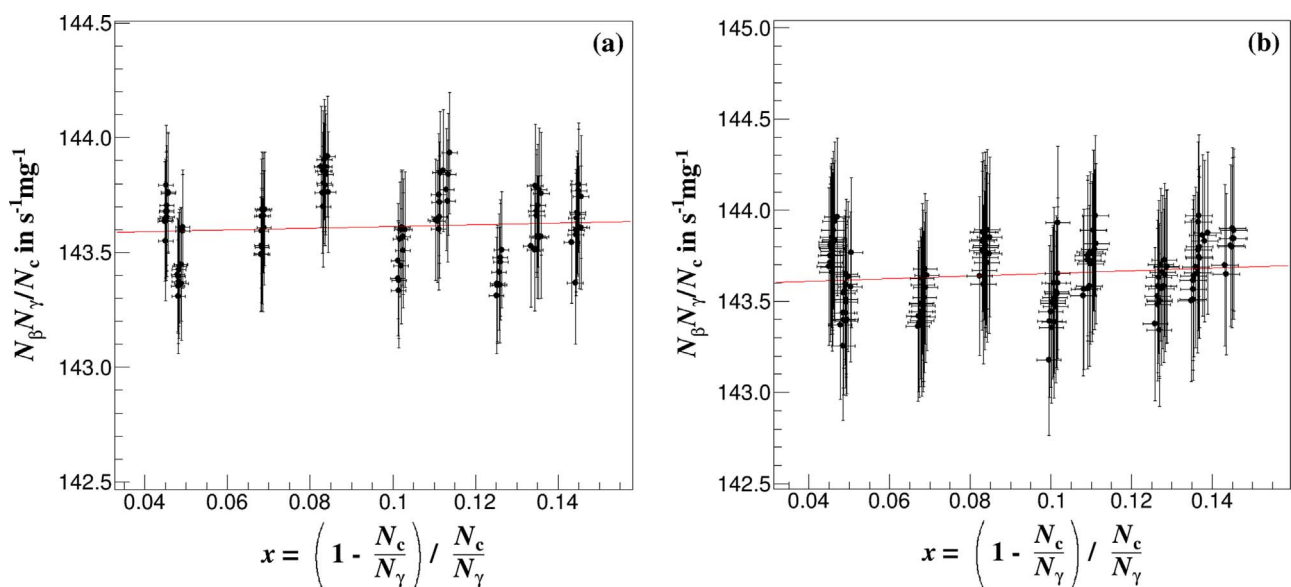
Fig. 4. $\frac{N_\beta \cdot N_\gamma}{N_c}$ measured with a 4πβ(PC)-γ coincidence system as a function of $x = \frac{\left(1 - \frac{N_c}{N_\gamma}\right)}{\left(\frac{N_c}{N_\gamma}\right)}$; function $f(x)$ is a 1st degree polynomial which was fitted to the experimental data, and the bars represent the statistical uncertainty of the individual data. In the left figure an open γ window was used, whereas the γ window was limited to the region of the two dominant peaks at 1173 keV and 1332.5 keV in the right figure.

Table 1
Activity concentration as determined from 4πβ(LS)-γ and 4πβ(PC)-γ coincidence counting using various extrapolation functions and experimental conditions.

Activity concentration (kBq g^{-1})	Coincidence counting method	γ-window setting	Fitting function
143.658	4πβ(LS)-γ with $N_\beta = N_D$	Full spectrum	2nd deg. polyn.
143.614	4πβ(LS)-γ with $N_\beta = N_T$	Full spectrum	2nd deg. polyn.
143.487	4πβ(LS)-γ with $N_\beta = N_D$	Peaks at 1173.228 keV and 1332.492 keV	2nd deg. polyn.
143.451	4πβ(LS)-γ with $N_\beta = N_T$	Peaks at 1173.228 keV and 1332.492 keV	2nd deg. polyn.
143.417	4πβ(LS)-γ with $N_\beta = N_D$	Peak at 1173.228 keV	2nd deg. polyn.
143.390	4πβ(LS)-γ with $N_\beta = N_T$	Peak 1173.228 keV	2nd deg. polyn.
143.675	4πβ(PC)-γ with G1	Full spectrum	1st deg. polyn.
143.576	4πβ(PC)-γ with G2	Full spectrum	1st deg. polyn.
143.593	4πβ(PC)-γ with G1	Peaks at 1173.228 keV and 1332.492 keV	1st deg. polyn.
143.581	4πβ(PC)-γ with G2	Peaks at 1173.228 keV and 1332.492 keV	1st deg. polyn.

Table 2
Uncertainty budgets for the activity concentration of the ^{60}Co solution measured by four methods.

Component	$u(a)/a$ in %			
	CIEMAT/ NIST	TDCR	4πβ (PC)-γ CC	4πβ (LS)-γ CC
Counting statistics	0.07	0.04	0.11[a]	0.06[a]
Weighing	0.03	0.03	0.05	0.02
Dead time	0.10	0.03	Negligible	0.20
Background	0.03	0.03	0.03	0.03
Resolving time	–	–	Negligible	0.20
Counting time	0.01	0.01	Negligible	Negligible
Adsorption	0.05	0.05	0.05	0.05
Decay correction	< 0.01	< 0.01	< 0.01	< 0.01
Extrapolation of efficiency curve	–	–	0.03	0.01
Impurities (no radioactive impurity detected)	< 0.03	< 0.03	< 0.03	< 0.03
^{3}H tracer activity and interpolation of efficiency curve	0.05	–	–	–
TDCR value and interpolation of efficiency curve	–	0.10	–	–
Model and decay data	0.16	0.12	Negligible	Negligible
Ionization quenching and kB value	0.07	0.07	–	–
PMT asymmetry	0.05	0.05	–	–
Fitting uncertainty (see text)	–	–	0.20	0.14
Square root of the sum of quadratic components	0.24	0.20	0.24	0.33

[a] correlations are taken into account.

former are realized by a delay line with increments of 2 ns while the latter are bound to the FPGA clock, resulting in a jitter and increments of about 5.882 ns. Further investigation may help to reduce these uncertainty components in the future.

4. Computation of the LS counting efficiencies and analysis of data for CIEMAT/NIST and TDCR

The LS counting efficiencies were calculated by means of the stochastic method (Grau Carles, 2007; Kossert et al., 2014) which also proved its worth for other β-γ isotopes (see, e.g., Kossert et al., 2012; Kossert and Nähle, 2014). The required input data such as energies of β and γ rays as well as the β decay probabilities were taken from the decay data evaluation project (DDEP) as published by Bé et al. (2006). Theoretical coefficients for internal conversion (IC) were recalculated with the conversion coefficient calculator BrIcc (v2.3 S) using the "frozen orbital" approximation (Kibédi et al., 2008), as IC values for L atomic subshells are not displayed in the DDEP tabulated data available

online. In the case of ^{60}Co, internal conversion occurs only during a very small fraction of decays and, consequently, the IC values are of minor importance. The ionization quenching function $Q(E)$ was calculated by means of the procedures described in a previous article (Kossert and Grau Carles, 2010).

Cobalt-60 decays by different β transitions (see Fig. 1). One of them is accompanied by the 1332.492 keV γ transition and the dominant branch is accompanied by both γ transitions with 1173.228 keV and 1332.492 keV, respectively. Thus, the computations were made for two cascades (pathways from ground state to ground state of the daughter nuclide).

The dominant β branch with a maximum energy of 317.32(21) keV and a probability of 99.88% is of an allowed nature. The β branch with a maximum energy of 1490.56(21) keV and a probability of 0.12% is of the unique 2nd forbidden type. The shape-factor function of the latter β transition was assumed to be $(W) = q^4 + \frac{10}{3}\lambda_2 q^2 p^2 + \lambda_3 p^4$. The λ_i parameters are energy-dependent and should be determined from relativistic electron wave functions. However, in this work $\lambda_1 = \lambda_2 = 1$ was applied. The importance of this beta spectrum to the calculation of the overall counting efficiency is rather small since the probability of this β branch is also quite small. In addition, the high maximum beta energy yields a high counting efficiency and lower sensitivity to variations of the beta spectrum.

The beta spectrum of the dominant allowed transition was calculated in various manners. At the beginning, the computation was carried out using the program routines from MICELLE (Grau Carles, 2007) and assuming a statistical shape factor, i.e. $C(W) = 1$. This computation yields the same spectrum as the LS analysis programs EFFY and CN2003 (Garcia-Toraño, Grau Malonda, 1985; Günther, 2002). In the following, this spectrum is referred to as the "classical" spectrum (dashed line in Fig. 5). The beta spectrum was also computed taking the atomic
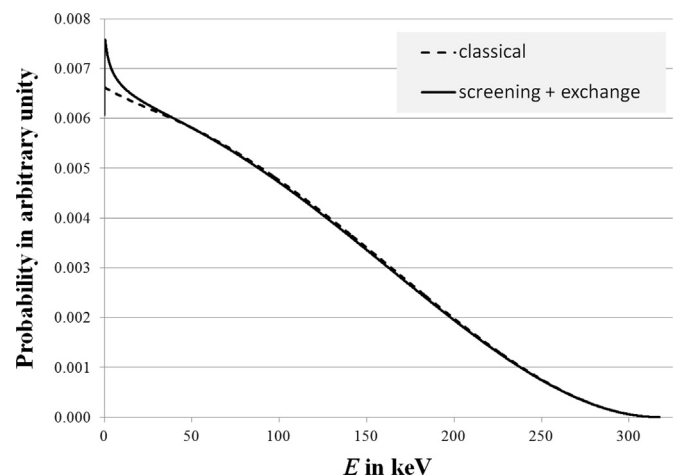

Fig. 5. Computed beta spectra for ^{60}Co. The "classical" spectrum (dashed line) was calculated without any correction, whereas the second spectrum (solid line) takes the atomic exchange effect and screening correction into account.
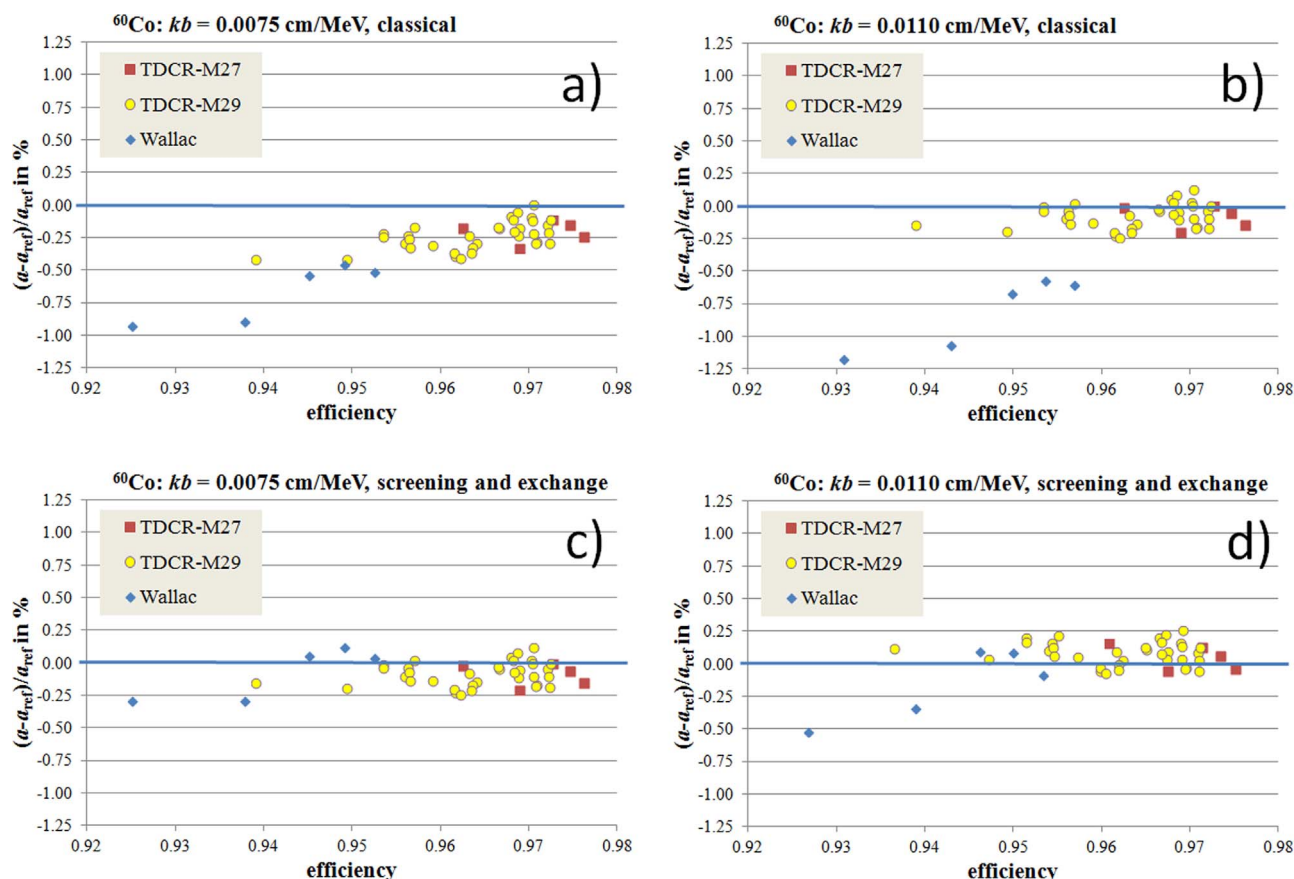
Fig. 6. Relative deviation between the activity concentrations determined from individual ^{60}Co LS samples and a reference value. The reference value ($a = 143.571$ kBq g^{-1}) was determined as the weighted mean of the two coincidence counting methods and is represented by the horizontal line at 0. The LS data were analysed with the following configurations: a) classical beta spectrum and $kb = 0.0075$ cm MeV^{-1}, b) classical beta spectrum and $kB = 0.0110$ cm MeV^{-1}, c) beta spectrum taking atomic exchange effect and screening correction into account and $kB = 0.0075$ cm MeV^{-1}, and d) beta spectrum as in c) and $kB = 0.0110$ cm MeV^{-1}.

exchange effect and screening corrections into account. The required electron wave functions for bound states and the continuum were calculated according to the approach described by Mougeot and Bisch (2014). The electron wave functions were then calculated numerically using the same screened Coulomb potential and a new screening correction was introduced. The atomic screening and exchange effects are therefore consistently accounted for.

This beta spectrum (solid line in Fig. 5) has a higher probability for low-energy electron emissions than the classical spectrum.

The LS data were then analysed using different combinations of beta spectra calculation and the kB parameter. The activity concentration obtained from all individual LS samples was calculated for each configuration. The results were then compared with the reference activity concentration $a = 143.571(35)$ kBq g^{-1}, which corresponds to the weighted mean of the two coincidence counting methods.

Fig. 6 shows the relative deviation between individual results of the LS samples and the reference value as a function of the ^{60}Co counting efficiency. At the beginning, the classical beta spectrum and a parameter $kB = 0.0075$ cm MeV^{-1} were used (Fig. 6a). The LS results are significantly lower than the reference value. The deviations increase at lower ^{60}Co counting efficiencies. It is to be noted that the activity concentration derived from the CIEMAT/NIST efficiency tracing is considerably lower than the results from TDCR. Such a discrepancy is an indication that wrong input data were used. Fig. 6b shows the result when using the same classical beta spectrum in combination with $kB = 0.0110$ cm MeV^{-1}. For this configuration, the TDCR results are in better agreement with the reference value. However, the discrepancies between the results from CIEMAT/NIST efficiency tracing and the other methods increase considerably.

Fig. 6c and d shows the residuals when using the beta spectrum with correction for atomic screening and exchange effects. In this case, the agreement between the LS methods and the reference value is very good. Again, the TDCR results increase slightly when changing the kB parameter from 0.0075 cm MeV^{-1} to 0.0110 cm MeV^{-1}, whereas the results from CIEMAT/NIST efficiency tracing decrease. A similar anti-correlation was found for many other isotopes (see, e.g., Nähle and Kossert, 2011). At PTB, $kB = 0.0075$ cm MeV^{-1} was found to be the best choice when using samples with 15 mL Ultima Gold and 1 mL of water. It is to be noted that the choice of the best kB parameter also depends on the parameterization of the electron stopping power.

In summary, the analysis shows that the results from TDCR and CIEMAT/NIST efficiency tracing are only in agreement when using the more sophisticated beta spectrum calculation, taking relevant corrections into account. In this case, both methods are also in agreement with the model independent reference value from the two coincidence counting methods.

The individual LS results were also used to calculate a mean value for the activity concentration. In this case, the results according to Fig. 6c were used, i.e. the beta spectrum with corrections and $kB = 0.0075$ cm MeV^{-1} were applied. The uncertainty budgets were determined following the guidance presented by Kossert et al. (2015) and are shown in Table 2. The dominant contribution to the overall uncertainty is assigned to decay data and the model. Here, it is taken into account that the state-of-the-art β spectrum calculation may still be imperfect. The influence of the ionization quenching function was investigated by changing the value of the kB parameter.

Table 3 also contains the individual results from the two TDCR counters. The relative deviation between these results is about 0.02%.

Table 3
Results for the determined activity concentration of the ^{60}Co solution under study (reference date: 1st June 2015, 0:00 CET). The final result corresponds to the weighted mean of the individual results from primary methods. A relative uncertainty of 0.20% was estimated for the final result. This uncertainty is larger than the internal (0.14%) and the external (0.05%) relative uncertainty of the weighted mean.

Method	a in kBq g^{-1}	Relative deviation from final result in %
Ionization chamber and dilution[a]	143.43(72)	− 0.042
TDCR (mean of results from 2 counters: 143.45 kBq g^{-1} and 143.48 kBq g^{-1})	143.47(29)	− 0.014
CIEMAT/NIST	143.44(35)	− 0.035
4πβ(PC)-γ coincidence counting	143.61(34)	0.084
4πβ(LS)-γ coincidence counting	143.50(47)	0.007
Final result	**143.49(29)**	–

[a] The result from the ionization chamber measurement is not taken into account for the calculation of the final result.

5. Combined result and discussion

The individual results of all four methods are shown in Table 3. The good agreement between the results supports usage of any of the four methods used in this work. It should, however, be emphasized that the liquid scintillation counting results require state-of-the-art computations of the beta spectrum. This work shows strong evidence for the necessity of taking screening effects as well as the atomic exchange effect into account. A similar finding was previously obtained from the liquid scintillation counting measurements of the pure beta emitter ^{63}Ni (Kossert and Mougeot, 2015). However, in the case of ^{63}Ni, there is no model-independent reference value from coincidence counting available and, hence, it is only possible to check consistency when varying efficiency and when comparing results of the TDCR method and CIEMAT/NIST efficiency tracing.

The current work also underlines the importance of 4πβ-γ coincidence counting as one of the most important primary activity standardization techniques. This method has a low model dependence and does not require any information about beta spectrum shapes.

The weighted mean of all four results from Table 3 $a =$ (143.49 ± 0.29) kBq g^{-1} is taken as the final result for the activity concentration. The uncertainty corresponds to the uncertainty from TDCR and is more conservative than usage of the internal or external uncertainty of the weighted mean. Correlations and anti-correlations between the results were not taken into account.

Acknowledgements

References

Bé, M.-.M., Chisté, V., Dulieu, C., Browne E., Baglin, C., Chechev, V., Kuzmenco, N., Helmer, R., Kondev, F., MacMahon, D., Lee, K.B., 2006. Table of radionuclides (Vol. 3 – A = 3 to 244). Monographie BIPM-5Vol. 3, Bureau International des Poids etMesures, Sèvres, ISBN-92-822-2218-7 and update at ⟨http://www.nucleide.org/DDEP_WG/DDEPdata.htm⟩, released 10 March 2010.

Bouchard, J., Cassette, Ph, 2000. MAC3: an electronic module for the processing of pulses delivered by a three photomultiplier liquid scintillation counting system. Appl. Radiat. Isot. 52, 669–672.

Broda, R., Cassette, Ph Kossert, K., 2007. Radionuclide metrology using liquid scintillation counting. Metrologia 44, S36–S52.

Garcia-Toraño, E., Grau Malonda, A., 1985. EFFY, a new program to compute the counting efficiency of beta particles in liquid scintillators. Comput. Phys. Commun. 36, 307–312.

Grau Carles, A., 2007. MICELLE, the micelle size effect on the LS counting efficiency. Comput. Phys. Commun. 176, 305–317.

Günther, E., 2002. What can we expect from the CIEMAT/NIST method? Appl. Radiat. Isot. 56, 357–360.

ICRU Report 52, 1994. Particle Counting in Radioactivity Measurements. Bethesda, Md., ISBN 0-913394-51-3.

Kibédi, T., Burrows, T.W., Trzhaskovskaya, M.B., Davidson, P.M., Nestor (Jr.), C.W., 2008. Evaluation of theoretical conversion coefficients using BrIcc. Nucl. Instrum. Methods A 589, 202–229. (And). ⟨http://bricc.anu.edu.au/⟩.

Kossert, K., Grau Carles, A., 2010. Improved method for the calculation of the counting efficiency of electron-capture nuclides in liquid scintillation samples. Appl. Radiat. Isot. 68, 1482–1488.

Kossert, K., Mougeot, X., 2015. The importance of the beta spectrum calculation for accurate activity determination of ^{63}Ni by means of liquid scintillation counting. Appl. Radiat. Isot. 101, 40–43.

Kossert, K., Nähle, O.J., 2014. Activity determination of ^{59}Fe. Appl. Radiat. Isot. 93, 33–37.

Kossert, K., Nähle, O., Grau Carles, A., 2011. Beta shape-factor function and activity deter-mination of ^{241}Pu. Appl. Radiat. Isot. 69, 1246–1250.

Kossert, K., Nähle, O.J., Ott, O., Dersch, R., 2012. Activity determination and nuclear decay data of ^{177}Lu. Appl. Radiat. Isot. 70, 2215–2221.

Kossert, K., Cassette, Ph, Grau Carles, A., Jörg, G., Lierse, V., Gostomski, Ch, Nähle, O., Wolf, Ch, 2014. Extension of the TDCR model to compute counting efficiencies for radionuclides with complex decay schemes. Appl. Radiat. Isot. 87, 242–248.

Kossert, K., Broda, R., Cassette, Ph, Ratel, G., Zimmerman, B., 2015. Uncertainty determination for activity measurements by means of the TDCR method and the CIEMAT/NIST efficiency tracing technique. Metrologia 52, S172–S190.

Loidl, M., Rodrigues, M., Censier, B., Kowalski, S., Mougeot, X., Cassette, P., Branger, T., Lacour, D., 2010. First measurement of the beta spectrum of ^{241}Pu with a cryogenic detector. Appl. Radiat. Isot. 68, 1454–1458.

Loidl, M., Rodrigues, M., Le-Bret, C., Mougeot, X., 2014. Beta spectrometry with metallic magnetic calorimeters. Appl. Radiat. Isot. 87, 302–305.

Marganiec-Gałązka, J., Nähle, O.J., Kossert, K., 2017. Activity determination of ^{68}Ge/^{68}Ga by means of 4πβ(Č)-γ coincidence counting. These Proceedings.

Mougeot, X., Bisch, C., 2014. Consistent calculation of the screening and exchange effects in allowed β- transitions. Phys. Rev. A 90, 012501.

Mougeot, X., Bé, M.-M., Bisch, C., Loidl, M., 2012. Evidence for the exchange effect in the β decay of ^{241}Pu. Phys. Rev. A 86, 042506.

Nähle, O., Kossert, K., 2011. Comparison of the TDCR method and the CIEMAT/NIST method for the activity determination of beta emitting nuclides. In: LSC2010, Advances in LS Spectrometry: Proceedings of the 2010 International Conference on LS Spectrometry, Paris, France, 6-10 September 2010, edited by Ph. Cassette, Radiocarbon, The University of Arizona, Tucson, Arizona, USA, ISBN 978-0-9638314-7-7, pp. 313–320.

Nähle, O., Kossert, K., Cassette, Ph, 2010. Activity standardization of ^{3}H with the new TDCR system at PTB. Appl. Radiat. Isot. 68, 1534–1536.

Nähle, O., Zhao, Q., Wanke, C., Weierganz, M., Kossert, K., 2014. A portable TDCR system. Appl. Radiat. Isot. 87, 249–253.

Schönfeld, E., Janssen, H., 1994. Precise measurement of dead time. Nucl. Instr. Methods A339, 137–143.

Schönfeld, E., Janssen, H., Klein, R., Hardy, J.C., Iacob, V., Sanchez-Vega, M., Griffin, H.C., Ludington, M.A., 2002. Production of Co-60 sources for high-accuracy efficiency calibrations of gamma-ray spectrometers. Appl. Radiat. Isot. 56, 215–221.

Smith, D., 1978. Improved correction formulae for coincidence counting. Nucl. Instrum. Methods 152, 505–519.